AN ABSTRACT OF THE THESIS OF

TADAO AOKI for the M.S. in MECHANICAL ENGINEERING
(Name) (Degree) (Major)

Date thesis is presented 11-23-65

Title THE STUDY OF ACTIVE SITES AND BUBBLE FORMATION FREQUENCY IN NUCLEATE BOILING HEAT TRANSFER

Abstract approved [redacted]
(Major professor)

The heat-transfer mechanism studied in this experiment was pool boiling from a flat horizontal surface facing upward with the bulk liquid at its saturation temperature. The hot-film anemometer probe was introduced to boiling heat-transfer analysis as a possible device for counting active nucleation sites and for other investigations such as measuring bubble frequency.

Although the existing hot-film probe had a high sensitivity to bubble motion, the strong agitation from the bubbles at the higher heat fluxes stripped the thin sensing film from the glass probe surface, indicating that some improvement on the hot-film probe was needed for it to be useful in boiling heat transfer analysis.

The largest heat flux examined was 113,300 B.t.u./(hr.)(sq. ft.) at which the measured density of active sites was 7,420/sq. ft. The correlation of active sites with the heat flux was represented by

$$q = 12.5 \left(\frac{n}{A}\right)$$

where q = heat flux, B.t.u./(hr.)(sq. ft.);

n = number of active sites;

A = heating surface area, sq. ft.

The statistical analysis of the three sets of data at heat fluxes of 45,800, 73,700 and 113,300 B.t.u./(hr.)(sq. ft.) showed that, at these heat-flux levels, the distribution of active sites followed the Poisson distribution within a five percent level of significance.

It was concluded that the hot-film probe was not an ideal device to measure bubble formation frequency because of the inability to detect bubble boundaries.

THE STUDY OF ACTIVE SITES AND BUBBLE FORMATION FREQUENCY IN NUCLEATE BOILING HEAT TRANSFER

by

TADAO AOKI

A THESIS

submitted to

OREGON STATE UNIVERSITY

in partial fulfillment of
the requirements for the
degree of

MASTER OF SCIENCE

June 1966

APPROVED:

Associate Professor of Mechanical Engineering
In Charge of Major

Head of Mechanical and Industrial Engineering

Dean of Graduate School

Date thesis is presented 11-23-65

Typed by Susan Carroll

ACKNOWLEDGMENT

My sincere appreciation goes to Dr. James R. Welty for his valuable suggestions throughout this project.

Also I would like to thank my typist, Susan Carroll.

TABLE OF CONTENTS

LIST OF FIGURES

Figure Page

THE STUDY OF ACTIVE SITES AND BUBBLE FORMATION FREQUENCY IN NUCLEATE BOILING HEAT TRANSFER

INTRODUCTION

The main objective of the present work is to introduce the hot-film anemometer to boiling heat-transfer analysis as a possible device for counting active sites and for other investigations such as measuring bubble formation frequency.

In spite of much study having been done recently in the boiling heat-transfer field, the mechanism of boiling phenomenon is not yet completely understood. The following description is to introduce the background of boiling heat transfer so that the present work can be better understood.

Boiling

It is well known that the boiling phenomenon consists of four different regions. For the sake of illustration, assume that an electrically heated surface is submerged in saturated liquid. Figure 1 is a typical curve of heat transfer coefficient, h, of the heating surface when it is plotted against a superheat temperature difference or the temperature difference between the heated surface and the bulk liquid, ΔT on a log-log scale graph.

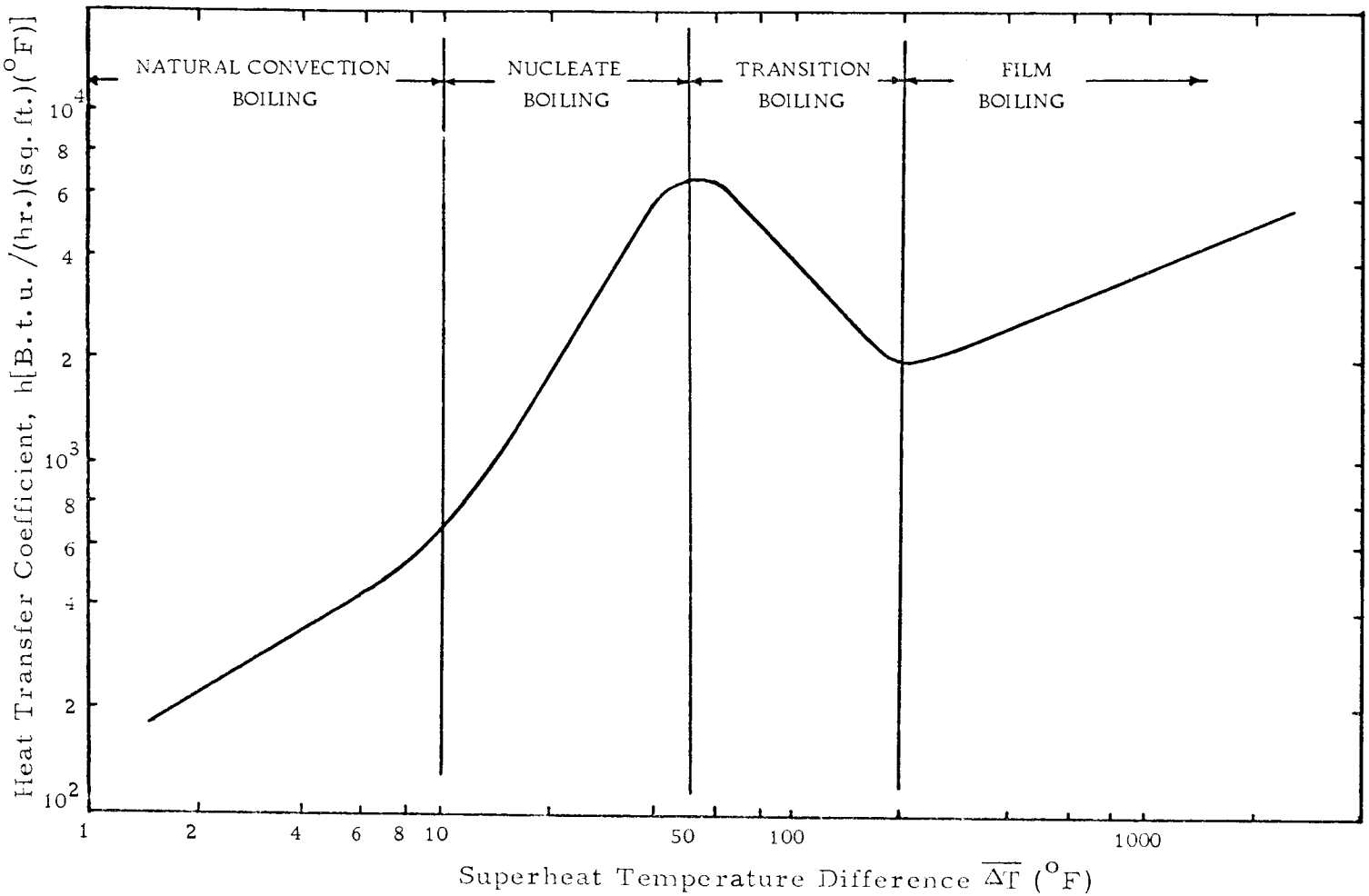

Figure 1. Heat Transfer Coefficient for Water Pool-boiling on Horizontal Tube at One Atmosphere

As the heat flux increases, the surface temperature rises and the liquid near the heating surface reaches a temperature slightly above saturation. Since the superheated liquid is less dense than the low-temperature saturated liquid, it tends to rise. In this region of boiling, the heat-transfer mechanism is simply natural convection and is thus called "natural convection boiling". Here bubbles form only on a few selected spots of the heating surface and rise in widely separated columns. The heat-transfer coefficient in this region is $0 < h < \sim$ 700 B. t. u. /(hr.)(sq. ft.)(^{o}F).

As the heat flux is increased the number of active nucleation sites, or spots on which bubbles start, becomes larger. The separation of bubbles from the densely populated heating surface and the interaction of bubbles above the surface cause considerable stirring action in the liquid which increases the heat-transfer rate. This region is called "nucleate boiling". Nucleate boiling has many important applications in industry because of its large heat transfer rates with a relatively small ΔT. As the heat flux is increased in the nucleate boiling region, more nucleation sites are activated and a vapor blanket begins to form. At some critical point the vapor blanket covers the entire surface and the heat-transfer mechanism changes completely. The heat-transfer coefficient at this point is approximately 6, 600 B. t. u. /(hr.)(sq. ft.)(^{o}F) as seen in Figure 1. This critical point is known as "burnout point". The exact knowledge of this point has great engineering importance

because the high heat flux is available to heat transfer equipment if it operates close to the burnout point.

Before a stable thin vapor film forms next to the heating surface, there exists a boiling region called "transition boiling" which is thought to be a combination of unstable film and unstable nucleate boiling alternating at a given location on the heating surface. It is interesting to note that with an increase in superheat temperature difference there is a decrease in the heat-transfer coefficient.

After h decreases to around 1,000 B.t.u./(hr.)(sq. ft.)(^{o}F), a stable thin vapor film forms next to the heating surface. This thin vapor film has a very low thermal conductivity and thus a large amount of the energy across this film must be transferred by radiation. This region is called "film boiling".

Nucleate Boiling

Nucleate boiling may be characterized by the formation of bubbles at preferred sites on a heating surface and a surface not fully covered by vaporfilm. The number of these active sites increases as the heat flux becomes larger. It is very important, therefore, to know how many active sites exist at a certain flux level and how they are distributed on a heating surface. A recent trend in nucleate boiling investigations has been to correlate the number of active sites with the heat flux. In past experiments the number of active sites

were counted visually. Because of a large number of active sites in a small heating area at high flux levels, it was not possible to count active sites at flux levels greater than 20,000 B.t.u./(hr.)(sq. ft.) for water, which is only about four percent of the maximum flux for nucleate boiling. The first and only successful active-sites counting has been reported by Gaertner and Westwater (4). Their technique for determining active sites consisted of plating a thin layer of nickel on a copper heating surface during the boiling runs and subsequently counting the number of pin holes in the plate. This electroplating method was used in aqueous solutions of nickel salts containing 20-percent solids in which boiling was achieved at atmospheric pressure on a horizontal, flat copper surface two inches in diameter. The maximum number of active sites thus counted was 1,130/sq. in. at 317,000 B.t.u./(hr.)(sq. ft.) or 60 percent of maximum flux.

LITERATURE REVIEW

Active Sites in Nucleate Boiling

One of the outstanding features of nucleate boiling is that bubbles usually select their active sites at specific locations on the heating surface. The prerequisite to boiling is the formation of a thin, considerably superheated layer of liquid on the heating surface and slight superheating of the bulk of the liquid. Clark, Strenge and Westwater (1) studied, quite extensively, the potential active sites by means of high-power electron micrographs and high-speed motion pictures and found that pits with diameters between 0.0003 and 0.003 inch were very active nucleate boiling sites. They also found that some scratches and residues of unidentified material were potential active sites.

The bubbles thus formed develop first by evaporation because of the considerable excess tempertaure of the liquid layer on the heating surface over the saturation temperature. The bubble breaks off when its volume has grown so much that its buoyancy exceeds the capillary forces which bind it to the heating surface (7).

When the bubble rises from a heating surface it carries away a quantity of energy q_b. Here the subscript b designates the break-off point, or the point on the heating surface from which a bubble rises. We may consider two types of heat transfer which are associated

with q_b. One is natural convection and the other is vaporization. The rate of heat transfer due to natural convection is, however, small enough to be negligible compared to that associated with the vaporization of liquid in nucleate boiling (14, 18). Thus, we may formulate q_b considering the vaporization of liquid only, i.e.,

$$q_b = h_{fg} G_b \qquad \text{(i)}$$

where q_b = heat transfer rate at the heating surface;

G_b = mass of a bubble;

h_{fg} = latent heat of vaporization.

If a bubble is approximated to be spherical in shape,

$$G_b = \rho_v V_b = \rho_v \left(\frac{\pi D_b^3}{6}\right) \qquad \text{(ii)}$$

where ρ_v = density of vapor bubble;

V_b = volume of a bubble:

D_b = diameter of a bubble.

Considering the static equilibrium between buoyant and adhesive forces Fritz (3) has obtained a single empirical relation between the volume V_b of a bubble when breaking off the heating surface, the outer contact angle β of the bubble at this instant, and the quantity called Laplace's capillarity constant, $\sqrt{\frac{2\sigma}{g(\rho_L - \rho_v)}}$.

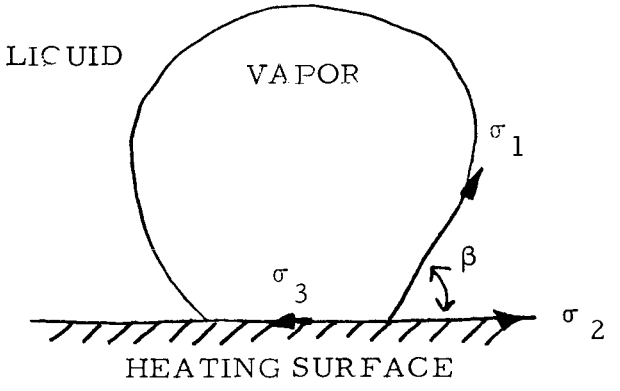

Figure 2. Surface-tension Forces Acting at the Point of Bubble Contact.

In the range from $\beta = 0$ to 140 degrees, this relationship can be expressed by the empirical equation

$$\sqrt[3]{V_b} \Big/ \sqrt{\frac{2\sigma}{g(\rho_L - \rho_v)}} = 0.0119\,\beta \qquad \text{(iii)}$$

$$D_b = 0.0209\,\beta \sqrt{\frac{\sigma}{g(\rho_L - \rho_v)}} \qquad \text{(iv)}$$

where g = acceleration of gravity;

σ = surface tension;

ρ_L = density of liquid;

ρ_v = density of vapor.

The total heat transfer rate q_b due to a number of bubbles is a function of bubble formation frequency f, the number of active sites per unit heating surface area, $\frac{n}{A}$, and the latent heat of vaporization h_{fg}. Hence,

$$q_b = h_{fg}\,\rho_v\,\frac{\pi D_b^3}{6}\,f\left(\frac{n}{A}\right) \qquad \text{(v)}$$

Jakob (7) observed that although the frequency

of bubble formation and the diameter are both varied randomly, their product remained approximately constant, i.e.,

$$(f)(D_b) = \text{constant.} \qquad \text{(vi)}$$

Rohsenow (16) made his analysis using equation (vi). He wrote equation (v) as follows,

$$q_b = [(f \cdot D_b)h_{fg}\rho_v \frac{\pi D_b^2}{6}] (\frac{n}{A}) \qquad \text{(vii)}$$

and noted that since the quantities inside the brackets are constants or are functions of the saturation pressure only, q_b varied linearly with active-sites density, $\frac{n}{A}$, at a given pressure. He expressed the total heat flux as

$$q = C_p q_b \qquad \text{(viii)}$$

where C_p is a constant which may be a function of pressure.

Kurihara and Myers (8) counted active sites on a three-inch-diameter copper heating surface and obtained the relationship for water as

$$q \sim (\frac{n}{A})^{1/3}. \qquad \text{(ix)}$$

They tested different surface roughness; polishing it with 4/0, 3/0, 2/0, 0, 1, 2, and 140-mesh carborundum and concluded that the degree of surface roughness had no effect on the above relationship.

A recent investigation by Gaertner (5) showed for boiling water on a two-inch-diameter copper heating surface, polished with 4/0-mesh carborundum, that

$$q \sim (\frac{n}{A})^{2/3}. \qquad \text{(x)}$$

Distribution of Active Sites

If, in the case of a liquid adjacent to a heat source, the heating surface is smoothly polished so that there is no preferred potential site for bubble formation due to surface imperfections, the resulting distribution of active sites will be random and statistical.

Gaertner (4), using the only available data (6), found that the local density of active sites for boiling water containing dissolved nickel salts, at fluxes of 200,000, 294,000 and 316,000 B.t.u./(hr.)(sq. ft.) fitted a Poisson distribution quite well.

Bubble Formation Frequency

The frequency of bubble formation is closely related to the size of a bubble: when the frequency is large, the bubble is small. Jakob observed that the product of frequency and the diameter was constant at relatively low heat flux (7). For both water and carbontetrachloride the value of the constant was found to be 7.7 cm/second.

Zuber (17) has proposed an equation describing the product of frequency and diameter in terms of fluid properties. He assumed the product to be proportional to the velocity of the rise of bubbles in a liquid, U_∞. He used the expression for the velocity obtained by Peeble and Garber (15),

$$U_\infty = 1.18\left[\frac{\sigma g(\rho_L - \rho_v)}{\rho_L^2}\right]^{1/4} \qquad \text{(xi)}$$

and found

$$(f)(D_b) = 0.59\left[\frac{\sigma g(\rho_L - \rho_v)}{\rho_L^2}\right]^{1/4} \qquad \text{(xii)}$$

where σ = surface tension between liquid and vapor;

ρ_L, ρ_v = density of liquid and vapor, respectively;

g = acceleration of gravity.

McFadden and Grassmann (12) found semiempirically that

$$(f)(D_b)^{1/2} = 0.56\left[\frac{g(\rho_L - \rho_v)}{\rho_L}\right]^{1/2} \qquad \text{(xiii)}$$

for a given fluid. Also, since at relatively low heat flux, $(\rho_L - \rho_v)$ is approximated by ρ_L,

$$(f)(D_b)^{1/2} = 0.56\,(g)^{1/2} = 17.5\,(\text{cm})^{1/2}/\text{sec.} \qquad \text{(xiv)}$$

with no dependence on fluid or vapor properties.

EXPERIMENTAL APPARATUS

Boiling Apparatus

Figure 3 shows the heater used in this work which consisted of a copper cylinder two inches in diameter. Boiling took place on the upper surface of the cylinder. Heat was supplied electrically through 39 inches of No. 20 gauge nichrome wire which was coiled around the copper cylinder. The total resistance of the nichrome wire was 1.9 ohm. A groove was made on the wall of the cylinder where the nichrome wire was embedded for better heat conduction and positioning of the heating element. An adhesive cement called "Insa-lute" was applied in the groove to insulate the heating element electrically. A 6 1/2 inch O. D., 1/8 inch thick circular brass fin was silver-soldered around the top of the copper cylinder to give support and also to provide a continuous nonboiling surface next to the surface on which boiling was taking place. The fin was supported by a 6 1/2 inch O. D. iron cylinder which also housed the heater. The space inside the cylinder and around the heater was filled with glass wool for thermal insulation. The length of the cylinder was such that the surface of the heater was seven inches from the bottom of the water tank.

Figure 4 shows the location of the thermocouples. In order to determine the average temperature of the heating surface, eight

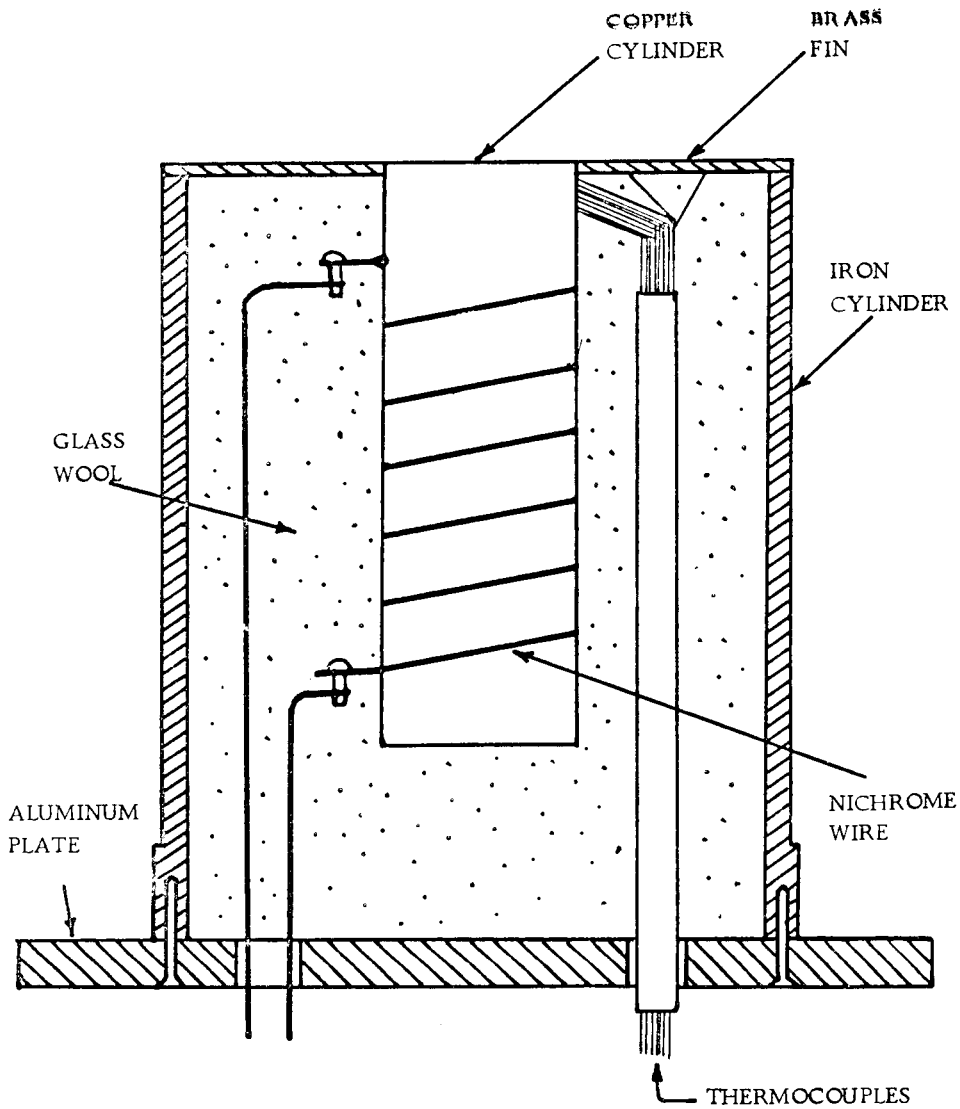

Figure 3. Heater and Its Housing

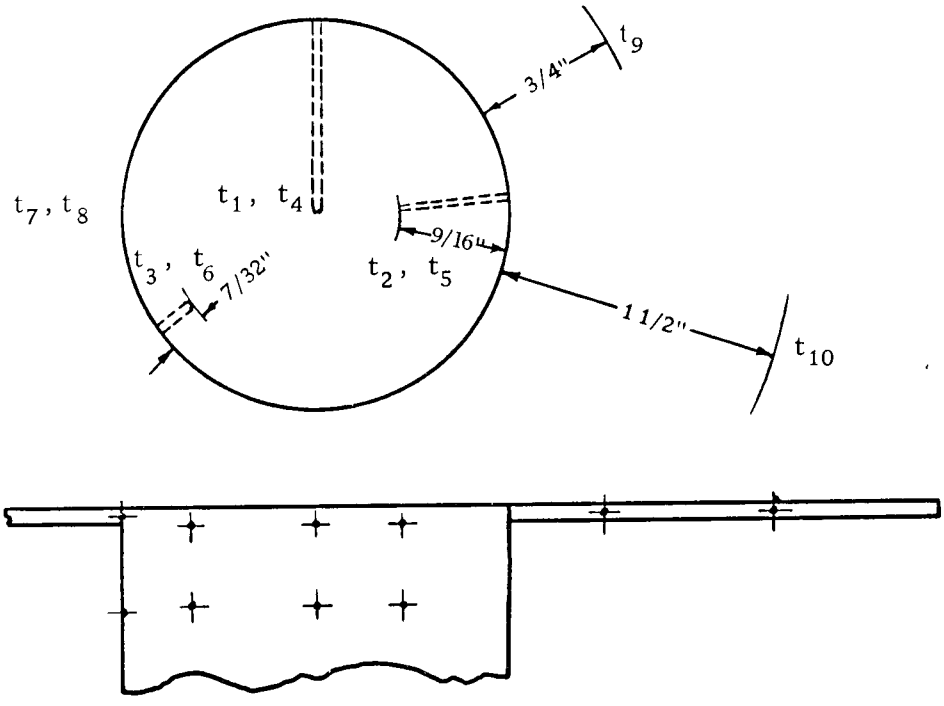

Figure 4. Location of Thermocouples

LOCATION OF THERMOCOUPLES IN COPPER CYLINDER

	DISTANCE FROM WALL	DISTANCE FROM SURFACE
t_1	1 inch	9/16 inch
t_2	9/16	9/16
t_3	7/32	9/16
t_4	1	3/16
t_5	9/16	3/16
t_6	7/32	3/16
t_7	0	5/8
t_8	0	1/4

LOCATION OF THERMOCOUPLES IN BRASS FIN

	DISTANCE FROM COPPER CYLINDER
t_9	3/4 inch
t_{10}	3/2

copper-constantan thermocouples were placed inside the copper cylinder. Three were located 3/16 inch below the heating surface at various distances from the axis of the heater; three others were at 9/16 inch directly beneath the first three thermocouples and two more were on the wall of the copper cylinder. Two thermocouples were also embedded in the fin to determine the heat loss from the fin to the water.

The aluminum tank in which boiling took place is shown in Figure 5. The 20 inch I. D. , 22 inch high cylindrical tank, with its inside surface painted, was filled with tap water. In order to keep the water at its saturation temperature, steam was run through a coiled copper tube which was immersed in the water. The amount of steam was controlled by means of a throttling valve. Three windows, four inches in diameter, were used for observation as well as picture taking of the boiling phenomenon. The outside of the tank was covered with glass wool in order to minimize heat loss by convection to air.

Figure 6 shows a schematic diagram of the electrical heater power-supply system. A 20-ampere capacity variac was used to adjust the 110-volt electrical power supply. The power input was measured using a voltmeter and an ammeter. Using a current transformer it was able to read three significant figures up to ten amperes.

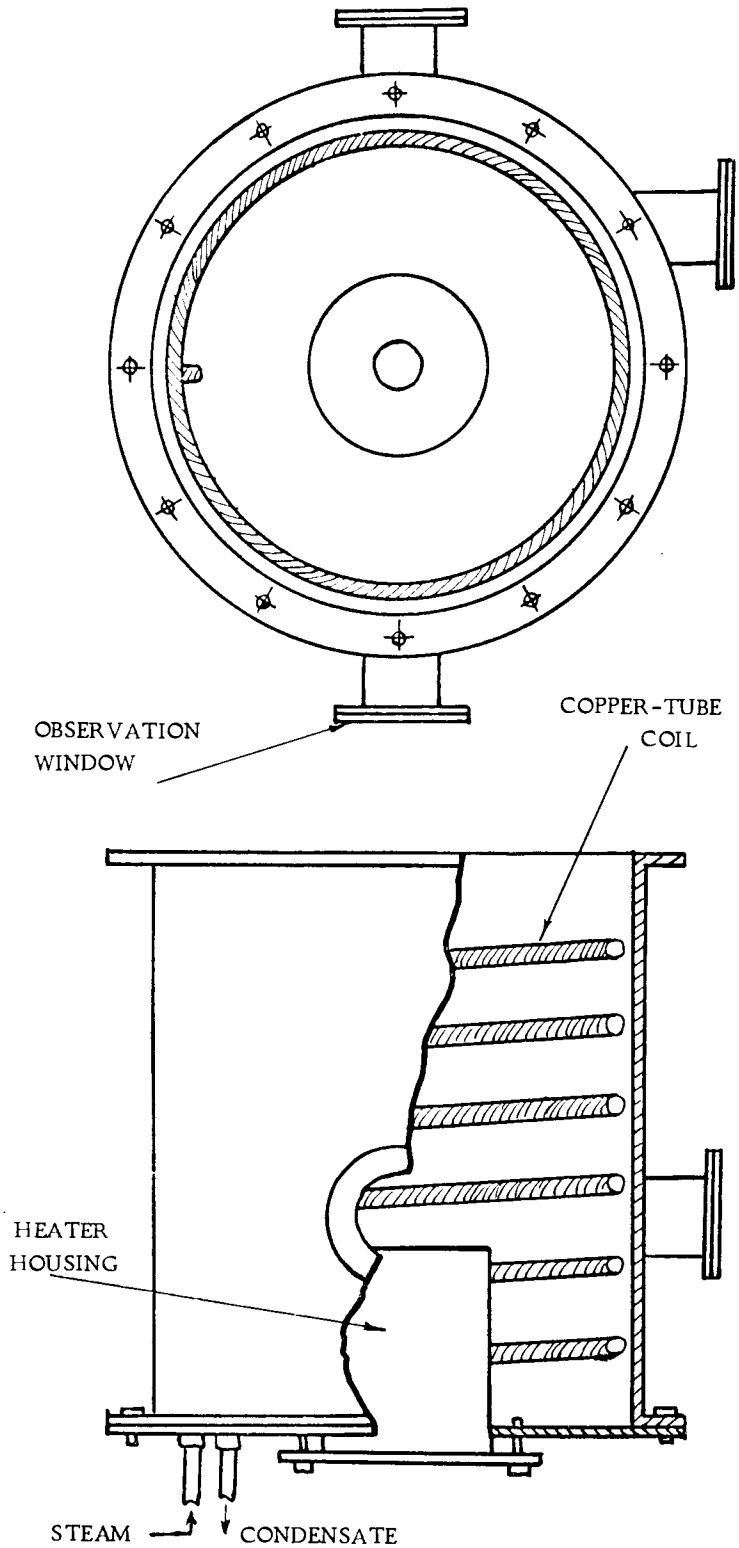

Figure 5. Boiling Tank

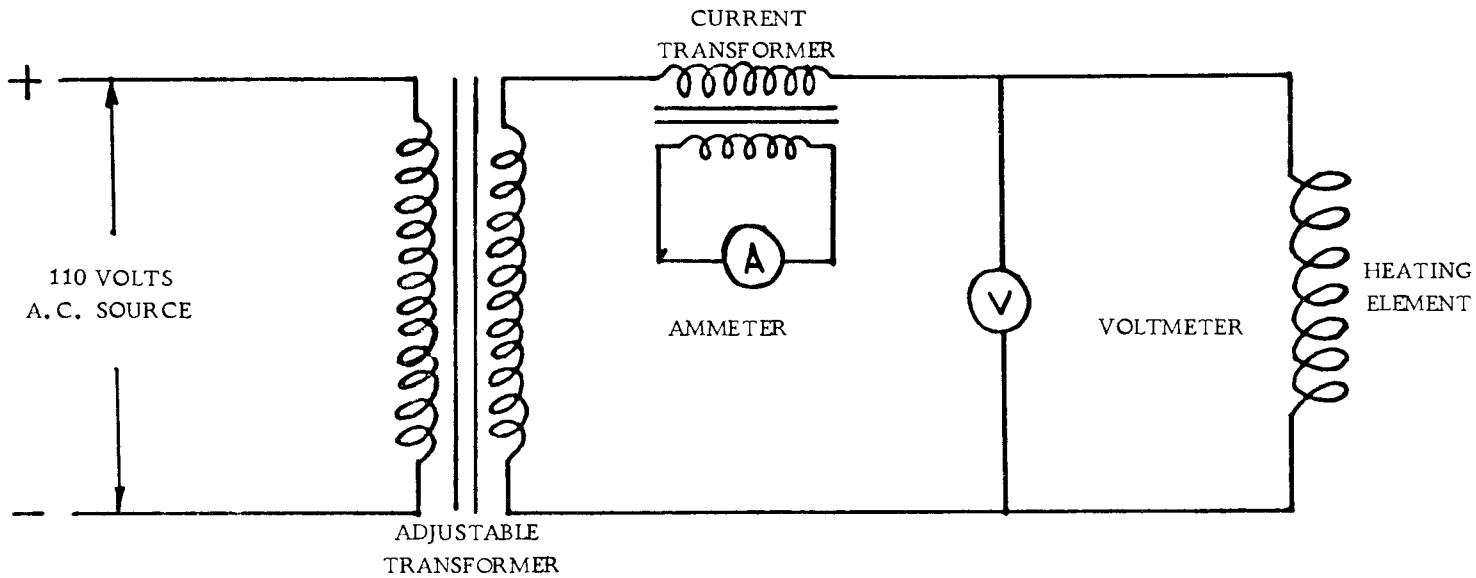

Figure 6. Heater Power Supply

Hot-film Anemometer

Data on bubble frequency and location were obtained using a hot-film anemometer probe, manufactured by Lintronic Laboratories, Ithaca, New York. The hot-film anemometer is similar in operation to the well-known hot-wire anemometer in which the rate of heat transfer from a sensing element is used to detect the characteristics of fluid motion. The sensing element for the hot-film anemometer is a thin platinum film about 50 to 100 angstroms thick, fused to the surface of a glass supporting structure. The probe is in the shape of a wedge, with the sensing element mounted on the tip of the wedge. Leads from the control circuit are connected to platinum leads in the glass probe body which emerge on the glass surface near the film. The film is connected to the platinum leads by means of a platinum sponge material; this sponge material serves as a good electrical conductor while at the same time permitting thermal expansion to occur between the glass and platinum film without breaking the electrical connection of film and leads (See Figure 7). The film is incorporated in a high response constant resistance feedback circuit.

The hot-film probe was mounted vertically above the heated surface using a positioning device as shown in Figure 8. The two micrometers made it possible for the probe to be positioned near the heating surface at a precisely known location.

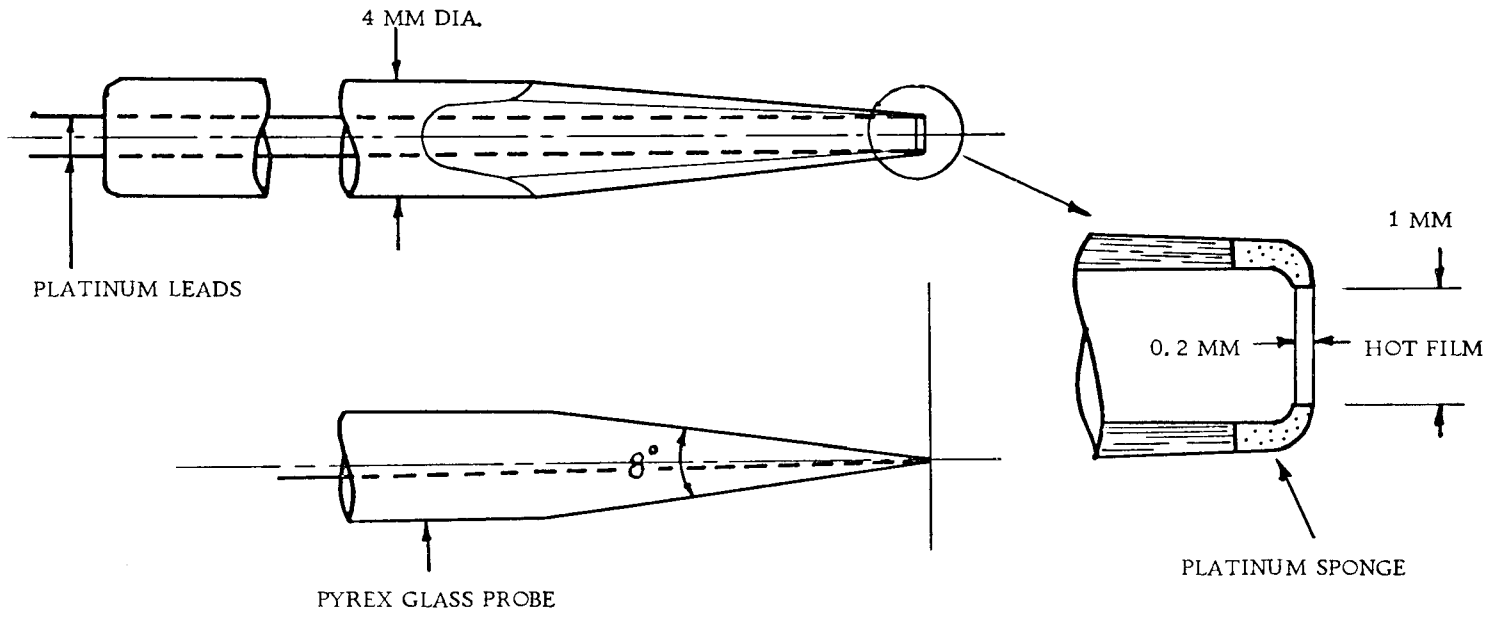

Figure 7. Hot-film Anemometer Probe

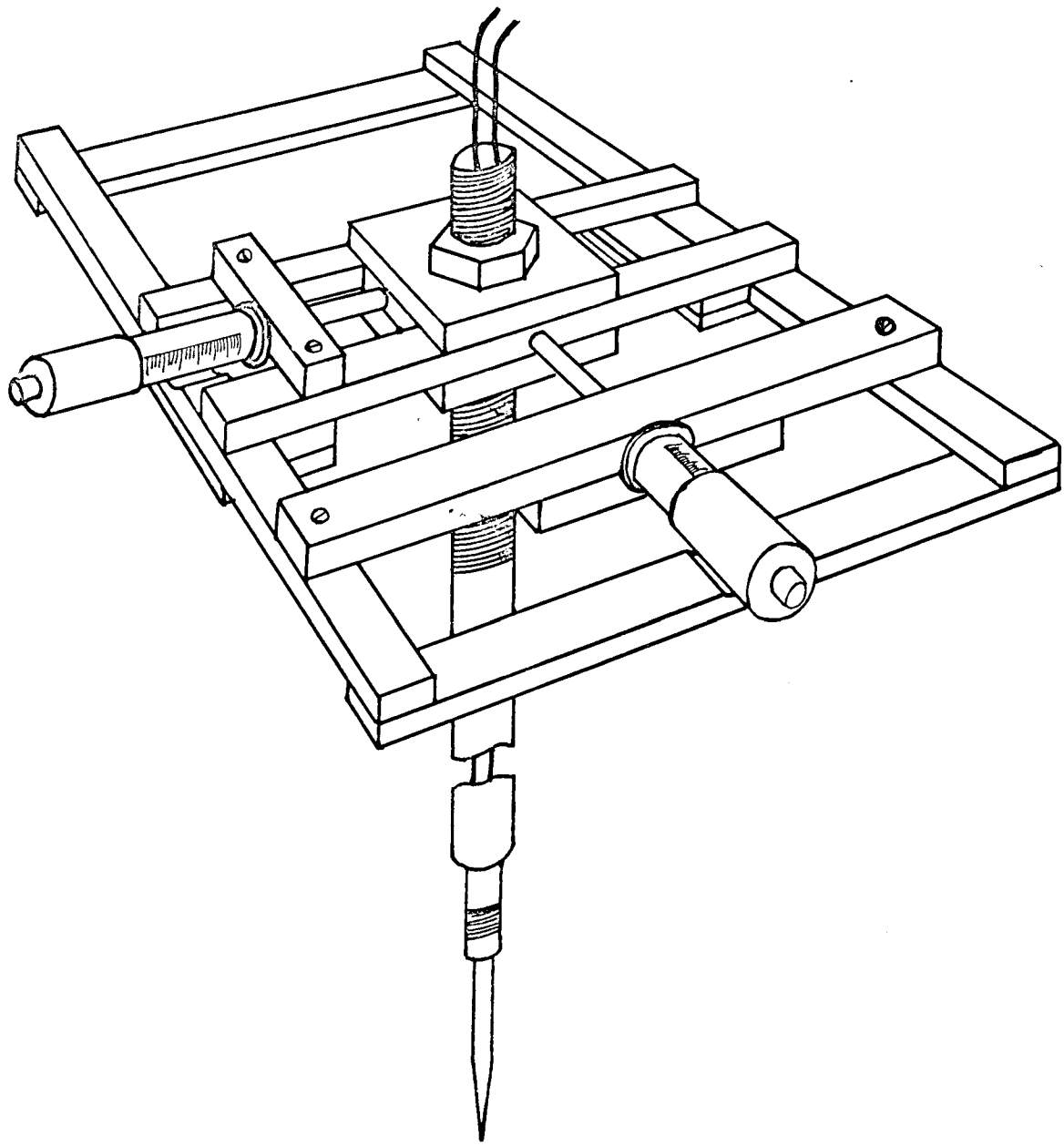

Figure 8. Hot-film Anemometer Probe and Its Positioning Device

EXPERIMENTAL PROCEDURES

Boiling Measurements

The heating surface was polished with No. 2 emery paper, then with 2/0 emery paper and finally with one-micron diamond powder placed on special paper for this purpose. The paper was wrapped around an aluminum rod and the polishing was done evenly in order to produce as uniform as possible surface.

The boiling tank was operated with the water level nine inches above the heating surface. For the system to reach thermal equilibrium the water had to be boiled vigorously for about two hours. Fifty-pound steam was used for this purpose as well as for keeping the bulk of the water at its saturation temperature during operation of the apparatus.

The water bulk temperature was measured with a mercury thermometer placed approximately 1/2 inch above the heating surface and also with a thermocouple for comparison purposes. Temperatures in the copper cylinder and brass fin were determined by thermocouples placed as shown in Figure 4.

The total heat input was determined from voltmeter and ammeter readings of the power supplied to the heater. The heat loss through the brass fin was calculated from the temperatures determined by the thermocouples embedded in the fin by a method to be

discussed in the next section. The ratio of fin loss to total heat input decreased rapidly as the latter increased, ranging from 25 to 2 percent in the nucleate boiling region. The heat transfer rate normal to the heating surface was obtained by subtracting the heat loss through the fin from the total heat input.

Active-sites Counting

During boiling, active sites were counted visually whenever possible. The hot-film anemometer was used at higher heat fluxes where the number of active sites was so great that a visual counting was not possible. The location of active sites was determined by the signal which was shown on the d. c. voltmeter of the anemometer-control panel. The anemometer signal was compared to visual indication at low fluxes to check its operation. A Sanborn recorder was also used for locating active sites.

Bubble Formation Frequency

To record the frequency at which bubbles formed the hot-film probe was placed in the center of a bubble column. The frequency of bubble rise was recorded on the Sanborn graph paper. At the same time an attempt was made to measure the bubble diameter or the diameter of a bubble column by moving the hot-film probe over the column and taking a micrometer reading while watching the d. c. voltmeter on the control panel.

METHOD OF ANALYSIS

Boiling Heat -transfer Curve

The heat transfer rate per unit area from the heated copper surface to the bulk of saturated water was plotted against the superheat temperature difference, that is, the temperature difference between the heated copper surface and the saturated water. Because of the heating mechanism the superheat temperature difference, ΔT, varied along the radius, r, of the heating surface. The mean value of ΔT or $\overline{\Delta T}$ was calculated from the following equation:

$$\overline{\Delta T} = \frac{1}{A}\int_A \Delta T \, dA = \int_0^1 \Delta T \, d\left(\frac{r}{r_0}\right)^2 \qquad \text{(xv)}$$

where r_0 is the radius of the heating surface with total area A. The surface temperature, T_s, was determined by a linear extrapolation of the temperatures measured in the copper cylinder. Then, $\overline{\Delta T}$ became the area under the curve of ΔT, i.e., temperature difference between the surface and saturated water, plotted versus $\left(\frac{r}{r_0}\right)^2$ as shown in Figure 9.

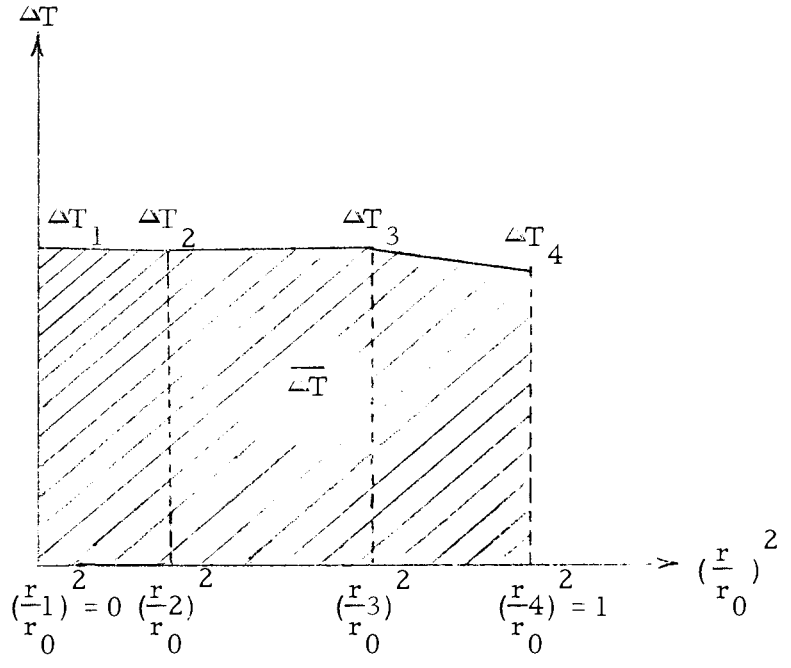

Figure 9. Local Superheat Temperature Difference vs. $(\frac{r}{r_0})^2$

The heat loss from the heater to the cylindrical fin by conduction was the major heat leakage existing in the present experiment. The steady-state heat conduction equation for a cylindrical fin of rectangular profile is

$$\frac{d}{dr}\left(A_r \frac{dT}{dr}\right) = \frac{hC}{k}\left(T - T_f\right) \qquad \text{(xvi)}$$

where T_f = fluid temperature;

C = periphery of a fin of radius $r = 2 \times 2\pi r$;

A_r = heat conduction area = $2\pi rb$;

b = thickness of a fin;

h = surface heat transfer coefficient.

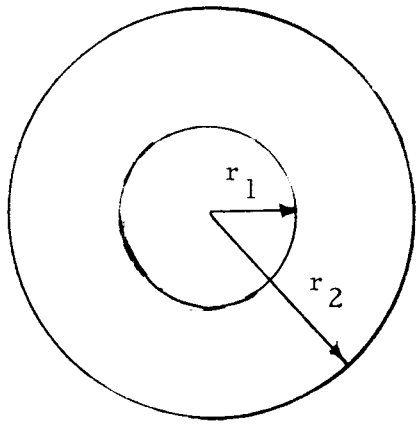

Figure 10. Cylindrical Fin

If the boundary conditions are taken as:

$$r = r_1;\ T = T_1$$
$$r = r_2;\ \frac{dT}{dr} = 0 \qquad \text{(xvii)}$$

then the solution to equation (xvi) is obtained in the form of modified Bessel functions.

$$\frac{T - T_f}{T_1 - T_f} = \frac{K_1(mr_2)I_0(mr) + I_1(mr_2)K_0(mr)}{K_1(mr_2)I_0(mr_1) + I_1(mr_2)K_0(mr_1)} \qquad \text{(xviii)}$$

where $m = \sqrt{\frac{2h}{kb}}$

K_0, K_1 = modified Bessel functions of the second kind of order zero and one respectively

I_0, I_1 = modified Bessel functions of the first kind of order zero and one respectively

The heat loss from the surface of a circular fin, q_L, one side of which is insulated, is

$$q_L = \int_{r_1}^{r_2} h_L A_r (T - T_f) dr = 2\pi \overline{h_L} \int_{r_1}^{r_2} (T - T_f) r dr \qquad \text{(xix)}$$

where $\overline{h_L}$ = the average value of surface heat-transfer coefficient.

From equation (xvi),

$$(T - T_f)r = \frac{1}{m^2} \frac{d}{dr}\left(r \frac{dT}{dr}\right) \qquad \text{(xx)}$$

substituting equation (xx) into (xix),

$$q_L = \frac{2\pi \overline{h_L}}{m^2} \int_{r_1}^{r_2} \frac{d}{dr} \left(r \frac{dT}{dr} \right) dr$$

$$= \frac{2\pi \overline{h_L}}{m^2} \left\{ r \frac{dT}{dr}\bigg|_{r = r_2} - r \frac{dT}{dr}\bigg|_{r = r_1} \right\} . \qquad \text{(xxi)}$$

The boundary condition eliminates the first term inside the bracket, thus,

$$q_L = - \frac{2\pi \overline{h_L} r_1}{m^2} \left(\frac{dT}{dr}\right)_{r = r_1} \qquad \text{(xxii)}$$

From equation (xviii) $\left(\frac{dT}{dr}\right)_{r = r_1}$ will be evaluated.

Hence,

$$q_L = \frac{- 2\pi \overline{h_L} r_1}{m} (T_1 - T_f) \left[\frac{K_1(mr_2)I_1(mr_1) - I_1(mr_2)K_1(mr_1)}{K_1(mr_2)I_0(mr_1) + I_1(mr_2)K_0(mr_1)} \right] \qquad \text{(xxiii)}$$

The convective heat transfer coefficient, h, was obtained from equation (xviii) knowing the properties of the fin material, its dimensions, and the temperature at a given position r. The experiment was done on a small piece of fin material (1 x 1/8 x 3 inches) to determine its thermal conductivity. Its value in the range of operating temperatures was found to be 63 B. t. u. /(hr.)(ft.)(^{o}F)

compared to table value of 75 B. t. u. /(hr.)(ft.)(^{o}F), (2). Local convective heat transfer coefficients, h, were determined at two points (t_9 and t_{10} in Figure 4) and their mean value, $\overline{h_L}$, was used to calculate q_L from equation (xxiii). A set of data was used to evaluate q_L following the method described above. The values of q_L/q_T were plotted against q_T, total heat input, as in Figure 11. Once this curve was plotted, it was possible to approximate q_L for the known q_T.

Spatial Distribution of Active Sites

A hypothesis was made that the spatial distribution of active sites fitted the Poisson probability distribution.

Certain physical phenomena, such as the number of bacterial colonies in plates of the same size or the number of diseased plants in plots of similar dimensions frequently follow this distribution. In physics the random emission of electrons from the filament of a vacuum tube, or from a photosensitive substance under the influence of light, and the spontaneous decomposition of radioactive atomic nuclei lead to phenomena obeying a Poisson probability distribution.

For the analysis of active-sites distribution, the area along the edge of the heating surface had to be excluded because of the excess active sites tending to form in this area. Because of this, the area of 2. 08 square inches or approximately 2/3 of the heating

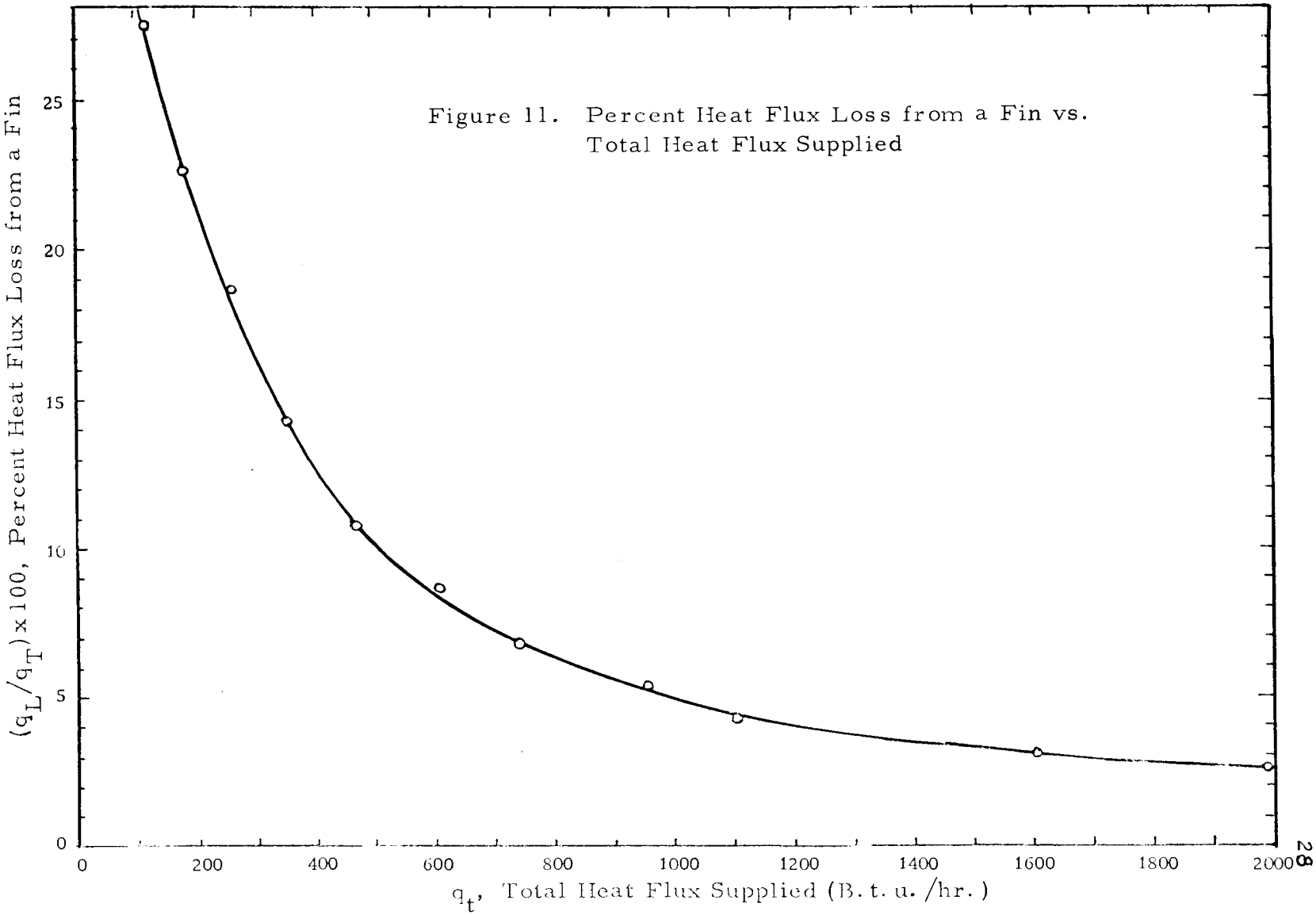

Figure 11. Percent Heat Flux Loss from a Fin vs. Total Heat Flux Supplied

surface, was taken as a test area where the surface was homogeneous and the active sites were distributed randomly. The test area was divided into 52 smaller areas or subareas, s, as shown in Figure 12.

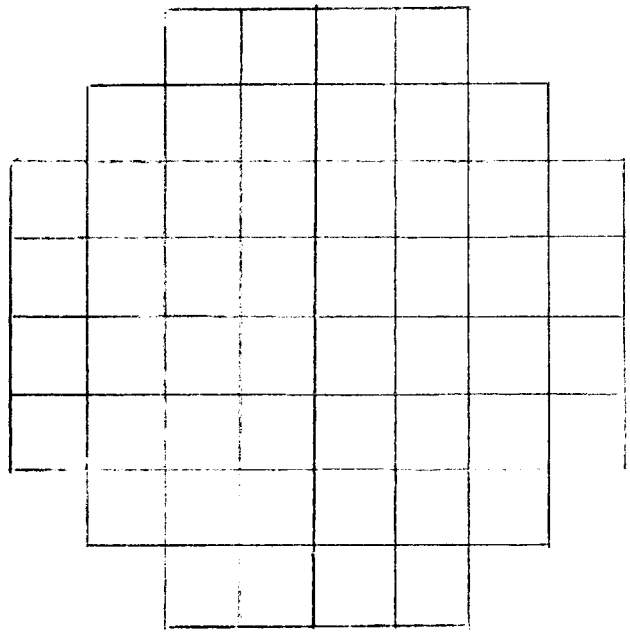

Figure 12. Active-sites Test Area: The Test Area was Divided into 52 Subareas.

The analysis was made in the following steps:

1. The construction of the frequency table--a frequency table consisted of (a) n, the possible number of active sites in a subarea s, (n = 0, 1, 2, . . .); (b) f, frequency or the number of subareas which had a specified number of active sites; and (c) r.f. relative frequency whose values were evaluated by dividing a particular frequency by a total frequency.

2. Histogram--a graph of a frequency table is called a histogram. For the present analysis f (frequency) was plotted against n (the possible number of active sites in a subarea).

3. Fitting histogram by Poissons probability curve.

If ξ is defined as the number of active sites in the subarea, s, of heating surface, $P_{\xi}(n; s)$ is the probability that in a single trial ξ is the given number n. If the hypothesis that the distribution of active sites follows the Poissons probability law is correct, $P_{\xi}(n; s)$ is given as (9),

$$P_{\xi}(n; s) = \frac{(ms)^n}{n!} e^{-ms} \quad \text{for } n = 0, 1, 2, . . \qquad \text{(xxiv)}$$

where m = the mean active sites in a subarea s.

The hypothetical frequency, h, was obtained from the Poisson distribution $P_{\xi}(n; s)$ i.e.,

$$h = (\sum_n f_n) P_{\xi}(n; s) \qquad \text{(xxv)}$$

The hypothetical frequency was compared with the observed frequency.

4. Chi-square (χ^2) test of goodness of fit.

This test involves finding the descrepancies between the observed frequencies f and the hypothetical frequencies h. Chi-square is defined as

$$\chi^2 = \Sigma \frac{(f-h)^2}{h} \qquad \text{(xxvi)}$$

It can be observed that the value of χ^2 is affected by the discrepancies (f-h). If this discrepancy is too large, the hypothesis must be

rejected. However, the rejected hypothesis may be actually true. The error made by rejecting a hypothesis that is actually true is called a type I error, and the probability of committing the type 1 error is called the level of significance. A χ^2 table gives the value of χ^2 for a known degree of freedom and for a chosen significance level. Thus, if the calculated χ^2 value is smaller than that given in the table, the hypothesis can be accepted with the chosen level of significance. In common practice five percent significance level is usually used (10).

RESULTS OF EXPERIMENT

Boiling Heat-transfer Results

The heat-transfer mechanism studied in the present experiment was pool boiling from a flat horizontal surface facing upward with the bulk liquid at its saturation temperature. The water was boiled on the mirror-like polished copper surface. The resulting heat-transfer data was shown in Figure 13 in small circles. The solid line is the result obtained by Gaertner (5) using similar boiling mechanism except his surface was polished with 4/0-mesh carborundum. It is seen that the data of present work agrees very well with the result of Gaertner. All the points obtained in the first nine runs were in the region left of the curve of Figure 13, indicating higher heat-transfer rates for a given temperature driving force. There were two reasons for this. The first reason was that after the heat flux was changed to a higher level, insufficient time was allowed for the heating system to reach its new equilibrium. Since, in this case, the temperature of the heating surface was lower than it should have been, the difference between this value and the saturation temperature of the water (superheat temperature difference, ΔT) was lower, thus the corresponding heat-flux density was higher causing the heat-transfer curve to be to the left of the true curve. The difference in the roughness of the heating surface was the second

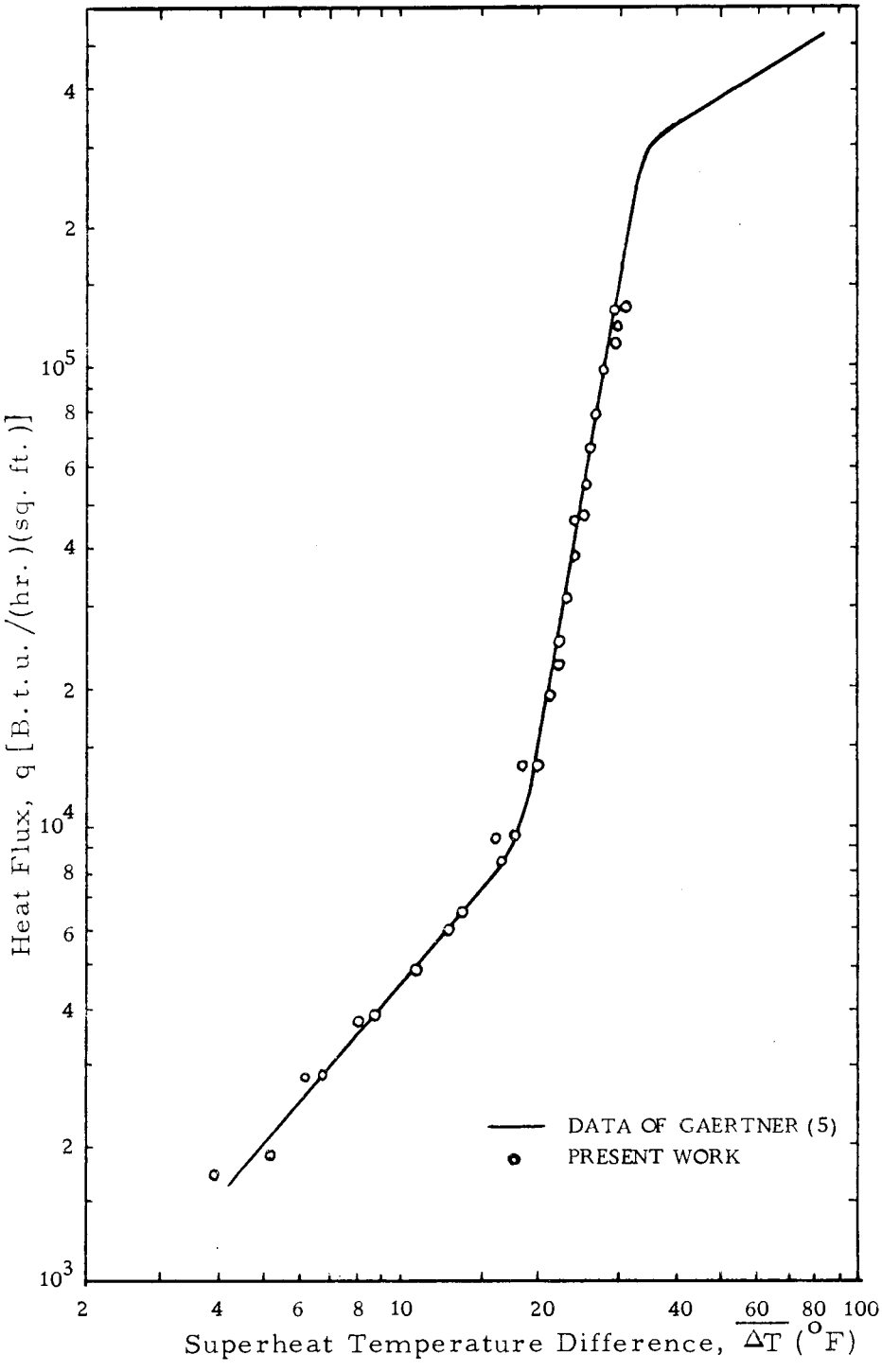

Figure 13. Heat Flux vs. Superheat Temperature Difference

reason why the first nine curves showed higher heat-transfer rate than normal. The heating surface had been prepared with 2/0 emery paper for each run. Later it was decided to polish the surface with a one-micron diamond powder. It is well documented in the literature for boiling heat transfer that the heat-transfer rate increases with an increase in the surface roughness (8). A separate test run was made to see the effect of surface roughness using No. 1-mesh carborundum. Figure 14 shows these results and a comparison with those using the mirror-like polished heating surface.

In Figure 13, two boiling regions are shown; the region for which the slope is moderate is one of natural convection boiling and the other is a nucleate boiling region. Nucleate boiling began to occur at a heat flux of 9,300 B.t.u./(hr.)(sq. ft.) and at a superheat temperature difference of 17.8°F. The relationship between superheat temperature difference and heat flux in this nucleate boiling was derived from the curve of Figure 13 as,

$$q = 2.71 \times 10^{-3} (\overline{\Delta T})^{5.22} \qquad \text{(xxvii)}$$

Since the curve is in log-log scales the exponent 5.22 of $\overline{\Delta T}$ is the slope of the line and the coefficient (2.71×10^{-3}) is the q-intercept of the line.

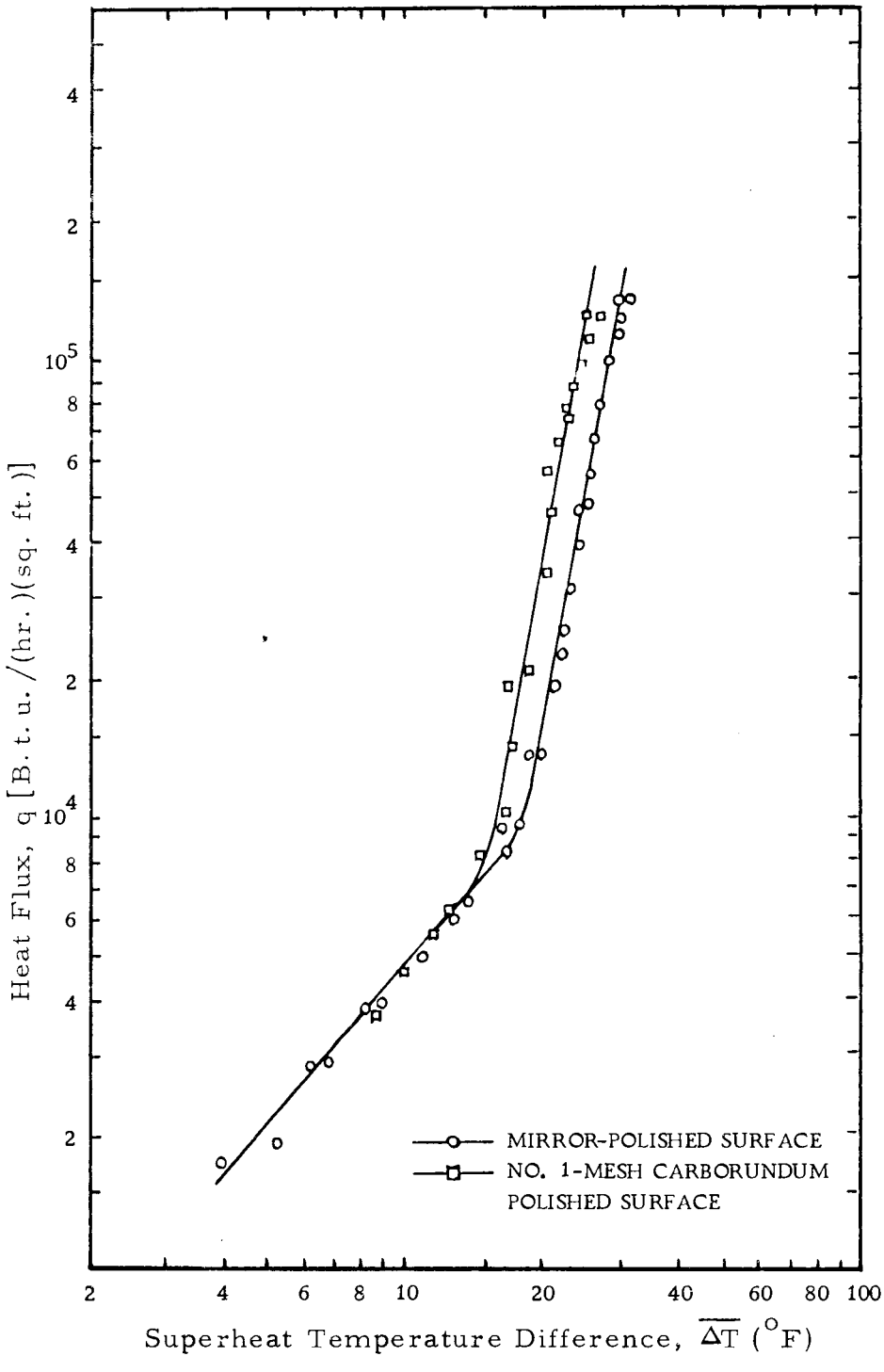

Figure 14. Effect of Surface Roughness on Boiling Heat Flux

Correlation of Active Sites and Heat Flux

The active sites were counted visually up to 16 in the test area or 1,110/sq. ft. at the heat flux of 13,570 B.t.u./(hr.)(sq. ft.). Beyond this heat flux, the location of active sites were determined by the hot-film probe. The signals from the probe were recorded on the Sanborn recording permapaper occasionally for confirmation purposes besides being read on the d.c. voltmeter on the anemometer-control panel. It was able to distinguish between active sites and non-active sites fairly well on the recording permapaper as seen in Figure 15. The largest heat flux examined was 113,300 B.t.u./(hr.)(sq. ft.) at which counts of active sites were 7,420/sq. ft.

Figure 16 shows the relationship between active nucleation sites and heat flux. It is seen that the transition from natural convection to nucleate boiling occurred at a flux of 10,600 B.t.u./(hr.)(sq. ft.) which is comparable to the value of 9,300 B.t.u./(hr.)(sq. ft.) found in Figure 13. The empirical correlation of active-sites density and the heat flux obtained in nucleation boiling was

$$q = 12.5 \left(\frac{n}{A}\right) \qquad \text{(xxviii)}$$

Thus, for the present boiling mechanism with the heating surface polished like a mirror, the heat flux varied linearly with active-sites density. For the similar boiling mechanism with the heating surface polished with 4/0 emery paper, Gaertner (5) reported that the

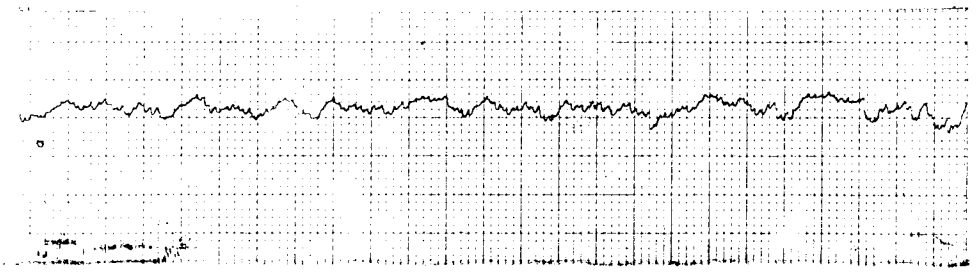

(a) NON-ACTIVE SITES

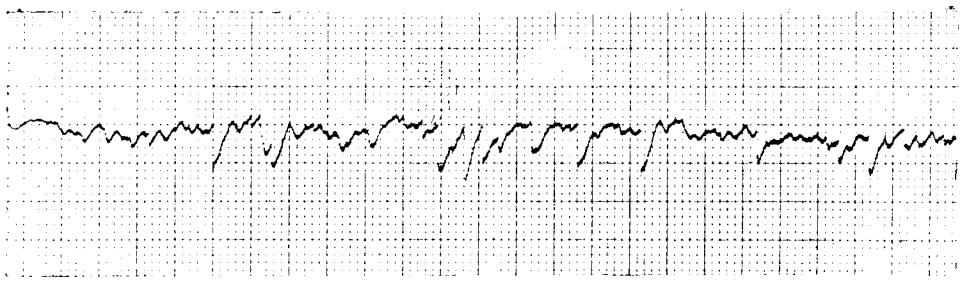

(b) ACTIVE SITES

q = 13,000 B.t.u./(hr.)(sq. ft.)

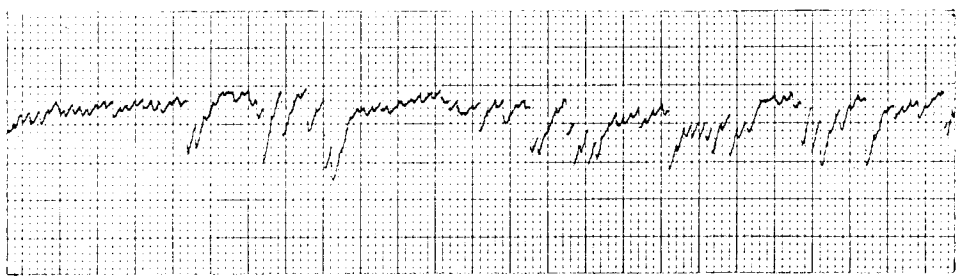

(c) ACTIVE SITES

q = 30,000 B.t.u./(hr.)(sq. ft.)

Figure 15. The Hot-film Probe Signals Recorded on the Sanborn Recording Permapaper

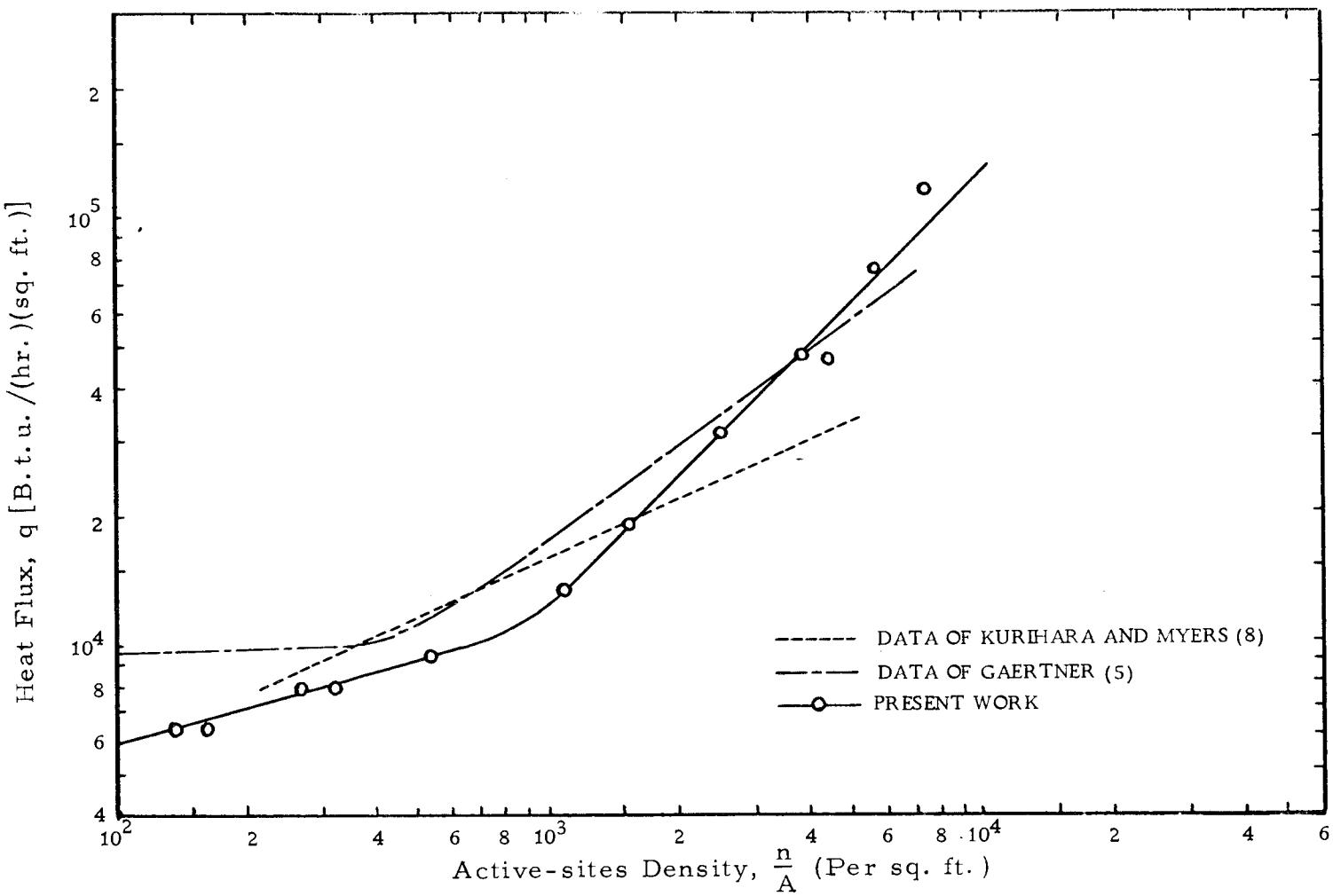

Figure 16. Heat Flux vs. Active-sites Density

exponent of $(\frac{n}{A})$ in equation (xxviii) was 2/3 rather than unity. Kurihara and Myers (8) obtained the value of 1/3 for the exponent $(\frac{n}{A})$ using the identical boiling system. Two explanations may be given as to why fewer active sites than those of the two references mentioned above were needed in the present experiment for the same heat flux. One is that the heating surface was smoother than the other two so that less active sites were formed for the given superheat temperature difference. The other is that greater agitation or mixing of bubbles and liquid may have occurred due to the heating-coil being located inside the water tank, causing the heat flux to increase without a corresponding increase in the number of active sites.

Spatial Distribution of Active Sites

It was observed during nucleate boiling that some of the active sites became inactive after a period of time had elapsed. It was also found that active sites left corrosion residue on the heating surface thus changing the nature of the surface. Therefore the active sites at a new heat flux were redistributed so that the new spatial distribution of active sites was independent of the previous one.

The hypothesis that the distribution of active sites follows the Poisson probability law was tested on the three sets of data that were previously taken in the present work for counting active sites. The heat fluxes of these sets of data were 45,800, 73,700 and 113,300

B. t. u. /(hr.)(sq. ft.). The spatial distribution of active sites on the test area, the tabulation of analysis, and the resulting values and their comparison with Poisson hypothesis are shown in Figures 17, 18 and 19. The Chi-square test made on the three sets of data showed that the hypothesis of Poisson distribution was acceptable within the significance level of five percent. The two more sets of data at lower heat fluxes (18, 950 and 31, 000 B. t. u. /(hr.)(sq. ft.) was not analyzed because the number of active sites was too small to give a statistical value.

Bubble Formation Frequency

Bubble formation frequency becomes meaningful when it is combined with the bubble diameter as seen in the Jakob's equation (vi). Hence, an effort was made to measure the diameter of a bubble with the hot-film probe. These values were not obtained. The finite size of the probe and the fact that the bubble does not rise straight but oscillates made it impossible to detect their boundaries. Probably the high speed motion picture camera is the best device for measuring bubble diameter and frequency simultaneously.

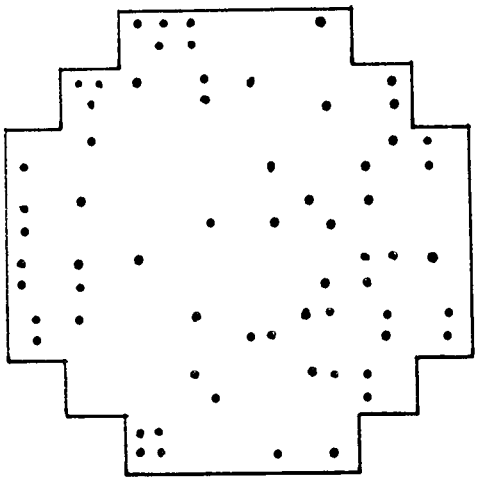

$\Sigma n = 65$

(a) DISTRIBUTION OF ACTIVE SITES

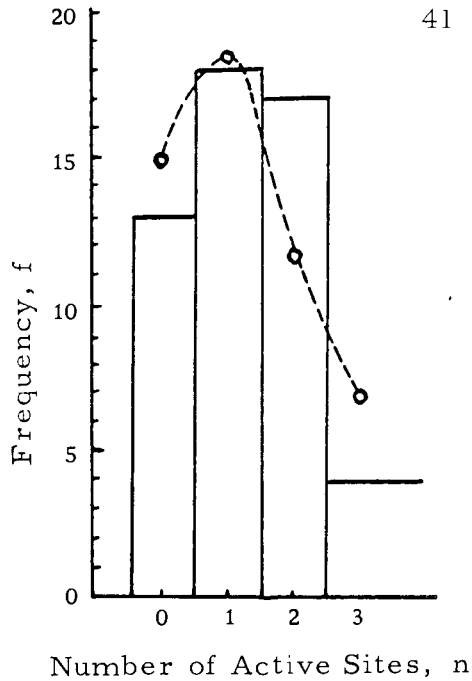

(b) HISTOGRAM AND POISSON DISTRIBUTION OF ACTIVE SITES

n	f	$P_s(n; s)$	h	(f-h)	$(f-h)^2$	χ^2
0	13	.287	14.93	-1.93	3.72	.249
1	18	.358	18.62	- .62	.38	.020
2	17	.224	11.65	5.35	28.6	2.452
3 or more	4	.131	6.82	-2.82	7.95	1.165
SUM →	52	1.000	52.02			3.886

Mean active sites in subarea, ms = 1.25

χ^2 within five percent significance level = 7.815

Figure 17. Spatial Distribution of Active Sites:
$\frac{q}{\Delta T}$ = 45,800 B.t.u./(hr.)(sq. ft.)
$\Delta T = 24.3^{\circ}F$

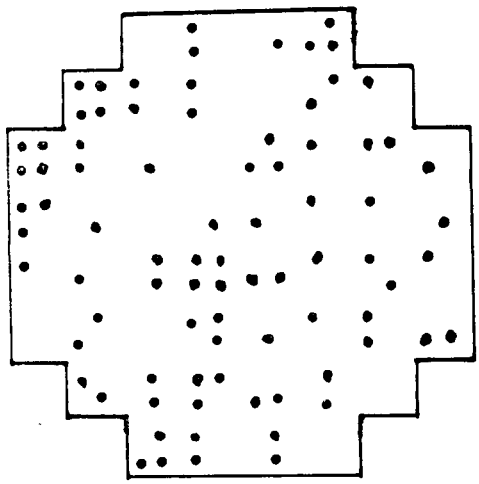

Σ n = 83

(a) DISTRIBUTION OF ACTIVE SITES

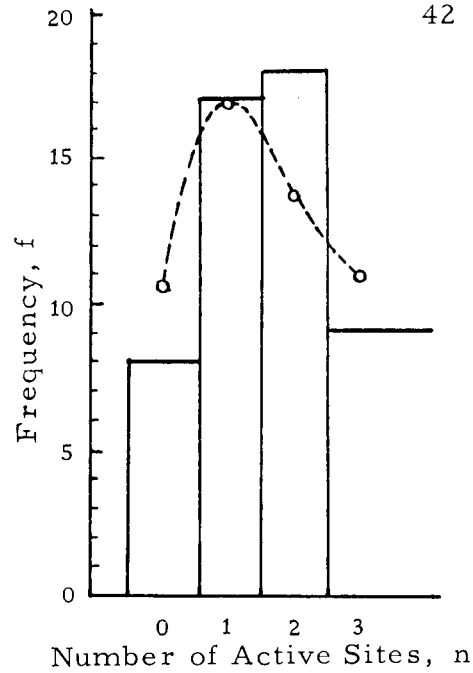

(b) HISTOGRAM AND POISSON DISTRIBUTION OF ACTIVE SITES

n	f	P_j (n; s)	h	(f -h)	$(f-h)^2$	χ^2
0	8	.203	10.57	-2.57	6.60	.624
1	17	.324	16.85	0.15	.02	.001
2	18	.258	13.42	4.58	20.98	1.562
3 or more	9	.215	11.20	-2.20	4.84	.432
SUM —	52	1.000	52.04			2.619

Mean active sites in subarea, ms = 1.60

χ^2 within five percent significance level = 7.815

Figure 18. Spatial Distribution of Active Sites:
$\frac{q}{\Delta T}$ = 73,700 B.t.u./(hr.)(sq. ft.)
ΔT = 26.5°F

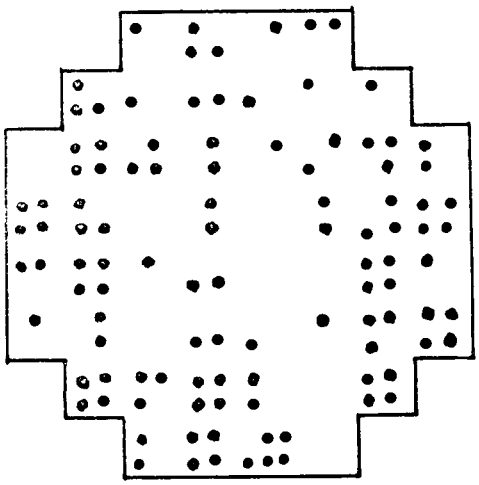

$\Sigma n = 107$

(a) DISTRIBUTION OF ACTIVE SITES

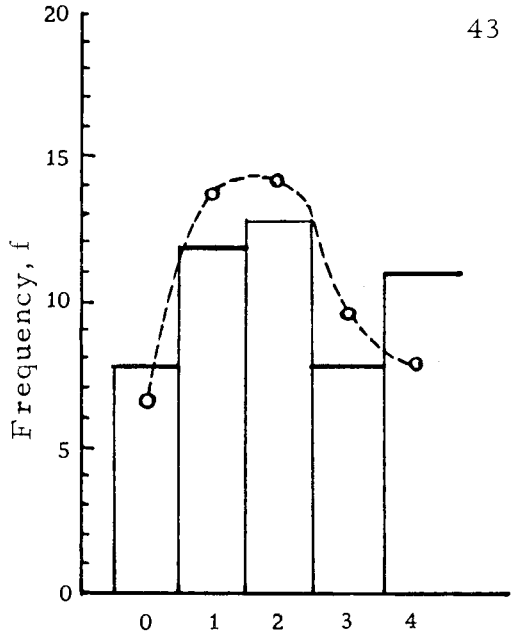

(b) HISTOGRAM AND POISSON DISTRIBUTION OF ACTIVE SITES

n	f	P_s (n; s)	h	(f-h)	$(f-h)^2$	χ^2
0	8	.128	6.65	1.35	1.82	.274
1	12	.263	13.70	-1.70	2.89	.211
2	13	.270	14.05	-1.05	1.10	.783
3	8	.186	9.67	-1.67	2.79	.289
4 or more	11	.153	7.96	3.04	9.24	1.162
SUM →	52	1.000	52.03			2.719

Mean active sites in subarea, ms = 2.06

χ^2 within five percent significance level = 9.487

Figure 19. Spatial Distribution of Active Sites:
$\frac{q}{\Delta T}$ = 113,300 B.t.u./(hr.)(sq. ft.)
$\Delta T = 29^{\circ}F$

SUMMARY

The major objective of the present experiment was to introduce the hot-film anemometer to boiling heat-transfer analysis as a possible device for counting active sites. It was found that the existing hot-film probe was highly sensitive to the motion of bubbles. However, twice during the course of the experiment the strong agitation from the bubbles at the higher heat fluxes stripped the platinum film from the glass probe surface. Although this was prevented by applying a thin film of print coating liquid to the hot-film probe, the resulting sensitivity decreased so much that it was no longer a suitable device for boiling analysis such as the measurement of bubble formation frequency. Another disadvantage of the existing hot-film probe is its size. If a needle-like probe were available, the active-sites counting would be much more accurate. The well-known hot-wire probe is a possible solution to this problem, but it is not sufficiently rugged to be used in boiling heat-transfer analysis. Certain modifications of the existing hot-film anemometer probe will make possible improved techniques for active-sites counting as well as other kinds of boiling heat-transfer measurements.

The statistical analysis of the three sets of data at heat fluxes of 45, 800, 73, 700 and 113, 300 B. t. u. /(hr.)(sq. ft.), showed that at these heat-flux levels the distribution of active sites followed the

Poisson distribution within a five percent level of significance. For the identical nucleate boiling mechanism as in the present work, Gaertner (5) also obtained the Poisson distribution for the active sites at heat fluxes of 200, 000, 294, 000 and 317, 000 B. t. u. /(hr.) (sq. ft.). Since the combined heat fluxes of Gaertner's and the present work cover most of the nucleate boiling regime, it may be concluded that the distribution of active sites in nucleate boiling follows the Poisson distribution.

Because of the finite size of the hot-film probe and the oscillatory motion of rising bubbles, boundaries of the bubble or bubble column were impossible to detect in the experiment. Also it was impossible to measure bubble formation frequency with the hot-film probe except at very low heat fluxes at which bubbles rose vertically and had definite boundaries.

RECOMMENDATION

It was found in the present work that the commercially available hot-film probe (Lintronic Laboratories, Ithaca, New York) was not an ideal device for boiling heat-transfer analysis; the strong agitation from the bubbles at high heat fluxes stripped the platinum film from the glass probe surface. This thin platinum film, about 50 to 100 angstroms thick is fused to the surface of the glass. The process used to fuse the metallic film to glass is first to dissolve platinic chloride and a suitable flux in an oil vehicle and then to apply this to the desired glass area and finally fire this at 530^{o}C. This operation causes the platinic chloride to be reduced to pure platinum fused to the glass surface (11). In order to solve the stripping problem of the thin platinum film, the fusion process must be studied in detail. Different materials than platinum may be fused better and used as sensing elements.

The reduction of the probe size in another problem. At Stanford University it was possible to make a cylindrical hot-film probe whose size was approximately 0.002 inch in diameter by 1/16 inch long (11). However, this probe was as fragile as a hot-wire probe. A probe ten times larger than the Stanford device would be sufficiently small for boiling heat-transfer analysis.

Besides modifying the existing hot-film probe, there may be

other sensing devices suitable for boiling heat-transfer analysis. Neal and Bankoff (13) devised an electrical resistivity probe capable of measuring local values of the volumetric gas fraction, bubble frequency, and local bubble size spectra. This probe consisted of a 1.25 inch steel sewing needle welded to the end of a six inch length of 0.033 inch steel wire. The probe was connected in series with a 1.5-volt battery and 10,000 ohm resistor and had a common ground with the conducting liquid. Thus, when the needle tip contacted liquid the circuit was closed; when it contacted gas the circuit was open. A disadvantage of this probe is that an ordinary liquid such as water wets the surface of the probe making it difficult to detect bubble boundaries.

In the present work the largest heat flux reached was around 120,000 B.t.u./(hr.)(sq. ft.) which is only about 24 percent of the maximum nucleate-boiling heat flux. This was due to the limited capacity of the variac avaiable. A future study should include the burnout point, thus covering the whole region of nucleate boiling.

For the identical boiling mechanism studied in the present work, Kurihara and Myers (8) concluded that neither the degree of surface microroughness nor the nature of the liquid had an effect on the following relationship between the heat-transfer coefficient and active-sites population:

$$h \propto \left(\frac{n}{A}\right)^{1/3} \qquad \text{(xxix)}$$

The result of Kurihara and Myers will be worth checking with the present boiling equipment. The surface roughness may be determined by the interference photomicrograph and the test liquids may include benzine, methanol, n-hexane, carbon tetrachloride or others.

Once the hot-film anemometer probe suitable to boiling heat-transfer analysis is made, the hydrodynamics of liquid motion above the boiling surface may be investigated, which may bring out new knowledge of the boiling phenomenon.

BIBLIOGRAPHY

1. Clark, H. B., P. S. Strenge and J. W. Westwater. Active sites for nucleate boiling. Chemical Engineering Progress Symposium Series 55(29):103-110. 1959.

2. Eckert, E. R. G. and R. M. Drake, Jr. Heat and mass transfer. New York, McGraw-Hill, 1959. 530 p.

3. Fritz, W. Berechnung des Maximalvolumens von Dampfblasen. Physikalische Zeitschrift 36:379-384. 1935.

4. Gaertner, R. F. Distribution of active sites in the nucleate boiling of liquid. Chemical Engineering Progress Symposium Series 59(41):52-61. 1963.

5. _____. Photographic study of nucleate pool boiling on a horizontal surface. Transactions of the American Society of Mechanical Engineering 87:17-26. 1965.

6. Gaertner, R. F. and J. W. Westwater. Population of active sites in nucleate boiling heat transfer. Chemical Engineering Progress Symposium Series 56(30):39-48. 1960.

7. Jakob, M. Heat transfer. New York, Wiley, 1949. 758 p.

8. Kurihara, H. M. and J. E. Myers. The effects of superheat and surface roughness on boiling coefficients. A. I. Ch. E. Journal 6(1):83-91. 1960.

9. Lee, Y. W. Statistical theory of communication. New York, Wiley, 1960. 509 p.

10. Li, J. C. R. Statistical inference. Vol. I. Rev. ed. Ann Arbor, Edwards Brothers, 1964. 658 p.

11. Ling, S. C. Heat transfer characteristics of hot-film sensing element used in flow measurement. Transactions of the American Society of Mechanical Engineers 82:629-634. 1960.

12. McFadden, S. W. and P. Grassmann. The relation between bubble frequency and diameter during nucleate pool boiling. International Journal of Heat and Mass Transfer 5:169-173. 1962.

13. Neal, L. G. and S. G. Bankoff. A high resolution resistivity probe for determination of local void properties in gas-liquid flow. A. I. Ch. E. Journal 9(4):490-494. 1963.

14. Nishikawa, K. and K. Yamagata. On the correlation of nucleate boiling heat transfer. International Journal of Heat and Mass Transfer 1:219-235. 1960.

15. Peebles, F. N. and H. J. Garber. Studies on the motion of gas bubbles in liquid. Chemical Engineering Progress 49(2): 88-97. 1953.

16. Rohsenow, W. M. A method of correlating heat-transfer data for surface boiling of liquids. Transactions of the American Society of Mechanical Engineers 74:969-974. 1951.

17. Zuber, N. Hydrodynamic aspects of boiling heat transfer. Ph. D. thesis. Los Angeles, University of California, 1959. 196 numb. leaves.

18. _____. Nucleate boiling: the region of isolated bubbles and the similarity with natural convection. International Journal of Heat and Mass Transfer 6:53-78. 1963.